CHAPTER 2.4

Brain Imaging and Synthetic PET

Amanda Bischoff-Grethe[1] and Michael A. Arbib[2]
[1]*Center for Cognitive Neuroscience Dartmouth College, Hanover, New Hampshire*
[2]*University of Southern California Brain Project and Computer Science Department, University of Southern California, Los Angeles, California*

Abstract

The advent of brain imaging techniques (PET, positron emission tomography; fMRI, functional magnetic resonance imaging) has led to new understanding of brain function. For the first time researchers can examine activation in the human brain not only during motor behavior, but also during cognitive behavior. Brain imaging has provided a way to study mental disorders and how various medications influence both function and activation. Unlike neurophysiological recordings of individual neurons where activity is recorded over milliseconds, imaging represents activation over a time period of seconds or even minutes. Knowing that the motor cortex was active during a particular task still does not tell us at what point the motor cortex was active, nor does it tell us the effect of excitatory and inhibitory connections to it. Synthetic PET was created as a way to bridge this gap by predicting functional activation based upon activity collected from models of brain function. Thus, it serves neuroscientists in multiple ways: it provides a way to validate models; it allows scientists to relate neuron activity to regional activation; and, finally, it allows us to study tasks which may normally be difficult to examine with traditional imaging or neurophysiological techniques. Synthetic PET therefore becomes a useful tool within the Neuroinformatics Workbench. In this chapter, we will discuss the Synthetic PET paradigm and provide examples of its function from models stored within BMW (Chapter 6.2). While our work to date has focused on the PET methodology, we stress that future work will pay increasing attention to fMRI data and the development of a corresponding methodology of Synthetic fMRI.

2.4.1 PET Imaging and Neurophysiology

Before delving into the methodology behind Synthetic PET, let us first review the biological basis of data collection in imaging. In brain imaging using PET, small doses of a radioactive tracer such as $H_2{}^{15}O$ water are injected into the subject prior to imaging during the performance of specified tasks. After a delay period of 10 to 20 seconds, the radioactive tracer reaches the brain. Its spatial distribution is determined using detectors sensitive to gamma photons generated by positron annihilation events. Typically, the first 45 to 90 seconds after injection of $H_2{}^{15}O$ produce a number of counts in each location which correlate almost linearly with the absolute regional cerebral blood flow (rCBF) (Herscovitch *et al.*, 1983; Raichle *et al.*, 1983). PET scans less than 45 seconds are usually not acquired, as the insufficient counts obtained are unable to overcome Poisson noise inherent in the detection method. In MRI, the subject lies within a strong magnetic field which causes the hydrogen atoms within his body to align their spin axes along the direction of the applied field. When brief pulses of radio waves are applied, the spin axes are perturbed; their spin axes tip away from their orientation with the magnetic field. When the pulse is turned off, the atoms realign with the magnetic field, releasing energy in the form of radio

Copyright © 2001 by Academic Press, Inc.
All rights of reproduction in any form reserved.

waves. These radio waves are the basis of the MRI image. The time interval used to acquire activity images varies among techniques: for PET, rCBF imaging is between 45 and 90 seconds; for fMRI at 1.5 Tesla using echo planar imaging (EPI), acquisition can be on the order of 1 or 2 seconds.

Neurophysiology operates on a different level. It is here that we use electrodes to study the firing pattern of individual neurons during a variety of tasks. Given the time course of the paradigm and the firing behavior of individual neurons, researchers can hypothesize not only how a brain region might be involved with a task, but also what the underlying cell populations may be doing in order to accomplish the task. In behavioral paradigms, neurons have been known to alter firing rates during pre-movement conditions, in expectation of reward, during movement, and at the end of movements. One can also determine the response of a neuron under varying neurochemical conditions; the application of an antagonist, for example, may affect the firing rate of a particular population of neurons. These responses are studied on the order of milliseconds, as opposed to up to several seconds in imaging. The drawback of neural recording, however, is that the explanation of the neuronal response is not clear in relation to the task at hand. A pre-movement neuron in one study may either be considered a predictor of behavior or an inhibitor of movement. There is also no true indicator that a population of recorded neurons represents a larger population with the same functional purpose. Conversely, the lack of a particular firing behavior does not mean it does not exist; it merely did not exist within the sample set. Still, neural recordings have greatly enhanced our understanding of brain function under various conditions. With the increasing popularity of computational models of neuronal behavior during task performance, activation patterns from similar tasks can be used to make predictions about behavior, leading to further experimental research.

Given these two methods of neuroscientific study, how, then, can we relate them not only to each other, but to computer models of neuron function as well? Despite the increased interest in brain imaging, it is still not clear exactly what the activations represent. It is impossible to distinguish excitatory and inhibitory cellular activity based on blood flow changes. After all, inhibition is an energy requiring task (Ackermann *et al.*, 1984). We also do not know the time course of the activation or how the individual neurons contribute to the activation, i.e., is activation due to pre-movement response or motor response in a brain area known to contain both? The purpose of Synthetic PET, then, is to attempt to bridge this gap and provide us with a mechanism for linking large-scale behavior with individual cellular behavior. Within the Neuroinformatics Workbench, Synthetic PET will allow us to visually compare behavioral responses of models stored within BMW to real imaging results and time series data.

2.4.2 Defining Synthetic PET

Synthetic PET is a technique by which neural models based upon primate neurophysiology are used to predict and analyze results from PET imaging taken during the performance of a variety of human behaviors. It is based upon the hypothesis that PET is correlated to the integrated synaptic activity within a region (Brownell *et al.*, 1982) and reflects neural activity in regions *afferent* to the region studied, rather than the intrinsic neural activity of the region alone.

Given the neural network representation described in the section "Building on Arrays of Neurons" of Chapter 2.1, the question is how to map the activity these networks simulate into predictions of activity to be recorded in corresponding regions within the human brain. There are two issues:

1. *Localization:* Each array within the neural network model represents a neural population that has been identified both physiologically and anatomically in the monkey. A Synthetic PET comparison requires explicit homologies (e.g., that region A_m in the monkey is homologous to region A_h in the human brain). (See Chapter 6.4 for details on how we determine homologies between species and how these homologies are stored within the database.) These regions should carry out the tasks under consideration in the same fashion. Sometimes the homology is well defined; at other times, its existence is not known. Thus, one of the aspects of Synthetic PET is to enable one to compare the results of a human brain study with those of a synthetic brain study, allowing one to test hypotheses of homologies across species. This in turn may lead to further studies to support or refute the claim.

2. *Modeling activation:* PET is said to measure rCBF. We hypothesized (Arbib *et al.*, 1995) that the counts acquired within PET scans may be correlated to local synaptic activity within a particular region, calling this the "raw PET activity." PET studies do not typically work directly with these values but rather with the comparative values of this activity within a given region during two different tasks or behaviors. We therefore define our computation in two stages:

a. Compute $rPET_A$, the simulated value of raw PET activity for each region A of the neural network while it is used to simulate the monkey's neural activity for a given task.
b. Compare the activities computed for two different tasks by "painting" this difference on the region A_h of a human brain (as represented by the Talairach Atlas; Talairach and Tournoux, 1988). The result is a Synthetic PET comparison presenting our prediction of human brain activity based upon a neural network model constrained by monkey neurophysiology and known functional neuroanatomy.

The *synthetic raw activity* $rPET_A$ associated with a cell group A is defined as:

$$rPET_A = \int_{t_0}^{t_1} \sum_B W_{B\to A}(t)dt, \qquad (1)$$

where A is the region of interest, the sum is over all regions B that project to the region of interest; $w_{B\to A}$ (t) is the synaptic activity (firing rate $\times$ | synaptic strength |) summed over all the synapses from region B to region A at time t; and the time interval from t_0 to t_1 corresponds to the duration of the scan.

The comparative activity $PET_A(1/2)$ for task 1 over task 2 for a given region is then calculated as:

$$rPET_A(1/2) = \frac{rPET_A(1) - rPET_A(2)}{rPET_A(2)}, \qquad (2)$$

where $rPET_A(i)$ is the value of $rPET_A$ in condition i. This allows us to compare the change in PET_A from task 2 to task 1. In the current study, we use a different measure, defining the change in *relative synaptic activity* for region A from task 1 to task 2, with $max(rPET_A(1), rPET_A(2))$ replacing $rPET_A(2)$ in the denominator of Eq. (2):

$$rPET_A(1/2) = \frac{rPET_A(1) - rPET_A(2)}{max(rPET_A(1), rPET_A(2))} \qquad (3)$$

This gives us a more robust measure of relative activity.

Synthetic PET results can be displayed in several ways, from using a graph or table to displaying the results on the region A_h homologous to A on a Talairach Atlas by converting the A values to a color scale. The resulting images then predict the results of human PET studies. Note, however, that we are displaying the *synaptic* activity of region A and not the neural activity of region A. As a computational plus, we may also collect the contributions of the excitatory and inhibitory synapses separately, based on evaluating the integrals in Eq. (1) over one set of synapses or the other. Using simulated PET we can tease apart the different factors that comprise the measure of synaptic activity for independent study. This can provide a more informed view of the actual PET data that are collected, possibly shedding light on apparent contradictions that arise from interpreting rCBF simply as cell activity.

2.4.3 Example: A Model of Saccadic Eye Movements

In order to demonstrate Synthetic PET, our example uses a neural network simulation originally designed by Dominey and Arbib (1992) for exploring how the cortex and basal ganglia interact with the superior colliculus and brainstem to produce a variety of saccadic movements. For the generation of a Synthetic PET we will concentrate on two kinds of saccades: *simple saccades*, in which the monkey fixates on a spot of light (the fixation point) that disappears upon the appearance of another spot of light (the target point) in another location, and *memory saccades*, in which the target point is briefly illuminated during the fixation period and the monkey saccades to the target's location upon removal of the fixation point. (See, for example, Hikosaka and Wurtz, 1983a,b, for details of simple and memory saccade studies in nonhuman primate.) We shall first briefly review the model (further details are provided in Chapter 2.1) before presenting the Synthetic PET comparing simple vs. memory saccades.

Model Description

Saccades are produced by the model via the interaction of neural networks representing the superior colliculus (SC), posterior parietal cortex (PP), frontal eye fields (FEF), the caudate (CD) and substantia nigra pars reticulata (SNr) of the basal ganglia, mediodorsal thalamus (MD), lateral geniculate nucleus (LGN), and the saccade generator of the brainstem (Fig. 1). These regions are further broken down into neuronal populations. Their interactions, both within a region and between regions, are responsible for generating succadic

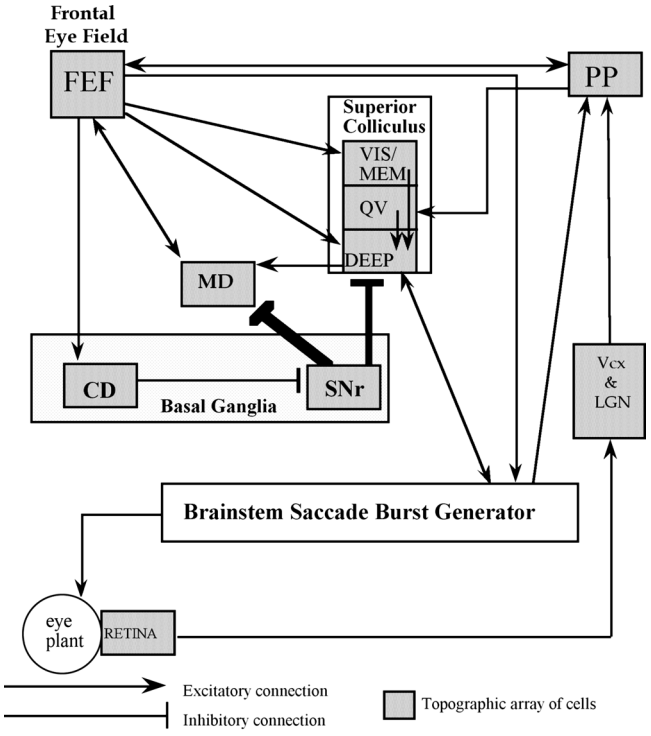

Figure 1 An overview of the Dominey and Arbib (1992) model of saccade generation. CD, caudate; DEEP, deep layer of superior colliculus; FEF, frontal eye field; LGN, lateral geniculate nucleus; MD, mediodorsal thalamus; MEM, superior colliculus memory cells; PP, posterior parietal cortex; QV, quasi-visual cells; SNr, substantia nigra pars reticulata; VIS, superior colliculus visual cells; Vcx, visual cortex.

behavior. The saccade generator performs a spatiotemporal transformation from the SC and FEF motor error maps, thus generating the eye movements needed to reposition the eye and hold it at a new vertical and horizontal gaze angle. For further details of the neurophysiology and the model constraints, please see Dominey and Arbib (1992).

The flow of activity through the model is as follows: The retina projects to PP cells via the LGN and the visual cortex and also provides input to the superficial superior colliculus (SCsup), a region that generates reflexive saccades to visual targets not recently fixated. PP codes future eye movements and has reciprocal connections with FEF and projections to FOn[AU4], cells which respond to visual stimulation of the fovea. Either FEF or SC activity is sufficient for commanding the execution of a saccade. FEF also projects to SC via the basal ganglia. The basal ganglia disinhibit SC and the thalamus for the purpose of saccades and spatial memory, respectively. CD receives projections from FEF which can trigger the release of SNr's inhibition of SC. The caudate and SNr provide an indirect link between FEF and SC, allowing FEF to selectively modulate the tonic inhibition of SNr on SC and thalamus via CD. The caudate contains a large number of neurons which are responsive to visual saccade targets and to remembered targets; the substantia nigra contributes to the dual inhibition of SC and the thalamus to allow cortex to selectively manage the inhibitory mask on SC via the FEF to CD pathway, thus preventing SC from evoking unintended saccades. Finally, SC applies a winner-take-all strategy to its various arrays, generating signals which convey the saccade metrics to the brainstem saccade generator.

Generating Synthetic PET

The Synthetic PET viewer is a Java JDK 1.2 applet designed to run within your current Internet browser. There are two main ways to generate Synthetic PET: (1) through the results generated by a NSL model within BMW, and (2) manually. In the first method, a NSL model, when executed, will automatically generate the synaptic data needed by Synthetic PET. Users planning to use the data at a later time must choose within BMW the option to save the data output within a database; this will store not only the time series data generated by the model but also the overall synaptic activity during the course of the trial (or trials). That is, during an experiment, the negative input, positive input, and overall input into a given region are saved. By saving these data separately, it allows us to view how negative and/or positive input determines the overall activation of a given region. Although we currently have manually coded the saccade model to generate the overall synaptic activity, there are plans for NSL itself to automatically calculate and save the synaptic activity for future use with Synthetic PET.

In order to use the synaptic data to paint atlas slices, the user need only select the "Generate Synthetic PET" option within BMW. The user will be queried as to which model to use. This will bring up an applet displaying the slices with the appropriate blobs of color, representing synaptic activation, within it. Users wishing to manually color the slices may do so using the controls along the top of the Synthetic PET viewer. To add a previously undefined ellipsoid to the display, the user presses the button titled "Add Blob." This button brings up a dialog box for entering in the required information. The user provides the region, the center coordinates of the ellipsoid, the ellipsoid's dimensions, an activation strength between 0.0 and 1.0 (correlated to the region with the maximum change in activation), and a color for display purposes. Pressing the submit button processes the entry, and the appropriate location of the atlas is colored.

We now consider the results generated by the saccade model. Using Eq. (3), the Synthetic PET viewer calculates the comparative data and determines the color and size of an ellipsoid. The size and center of the ellipsoid are based upon neurological data. The ellipsoid color is generated from Eq. (2); a negative change in activation correlates with a green ellipsoid, while a positive change in activation correlates with a red ellipsoid. This ellipsoid is then centered on coordinates based upon the homologous region in the human, A_h's location in the Talairach Atlas (Fig. 2; see color insert). The Synthetic PET viewer assumes the user wishes to display all regions represented within the model and for all connections (both positive and negative). In our example, areas showing activation increases are in red; areas decreasing their activation are green. The values computed from Eq. (3) are FEF: -23.6%; CD: 142.8%; MD: -10.5%; PP: 257.9%; SC: -22.0%; SNr: 208.2%; Vcx: 2.8%. The full color range of the blobs corresponds to $\pm 257\%$. Because PP has the largest change in activation, we correlate this range with the highest intensity of color. That is, if the color intensity were to range from 0 to 1, PP would have an activation strength of 1.0, whereas FEF, which has a lower change in activation, would have an activation strength of 0.09. By pressing a mouse button over a blob, the user can view the Talairach coordinates, the name of the region, and its activation strength (Fig. 3; see color insert). Pressing the mouse button over any area within a slice will always return the Talairach coordinates of the mouse pointer. If the user wishes to view a slice more closely, double clicking the mouse over the slice will add a new display with a larger view of the chosen slice. This is particularly helpful when examining a slice that contains several blobs of activity. The user may have multiple frames open at any given time.

The user may choose to manipulate the data being displayed in various ways. Because the current method of highlighting a region is an ellipsoid which may overlap into other regions, the user may hide or show individual ellipsoids. To do so, the user must first ensure that the

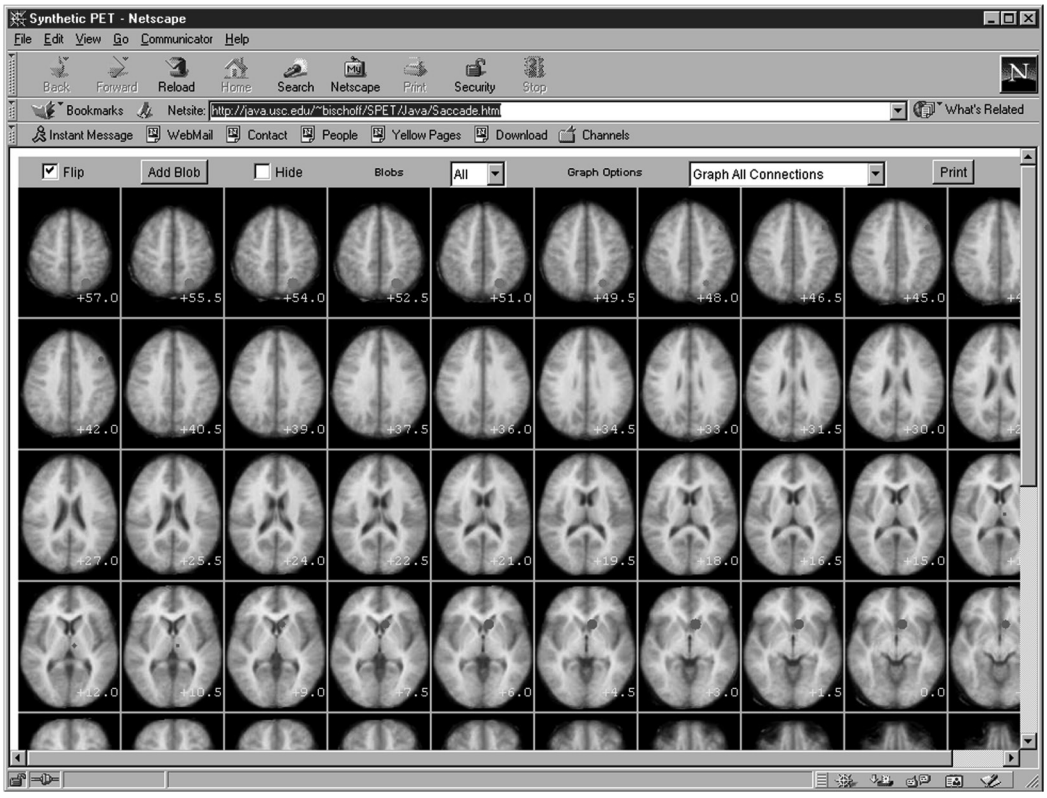

Figure 2 Synthetic PET comparison generated for the saccadic movement model. The top portion of the frame provides a checkbox for flipping the atlas orientation, adding new blobs, viewing or hiding specific blobs, and for choosing graph options. In the saccade example, we have chosen to view all the blobs and activation changes related to both positive and negative synaptic input. Red activation: overall increase in activity. Green activation: overall decrease in activity. (see color plates.)

checkbox on the toolbar marked "Hide" has been checked. To the right of the checkbox is a pull-down menu of all the blobs that exist in the dataset. These include both the blobs of activation input from the database and those the user has hard coded using the "Add Blob" dialog. The user chooses the blob to hide, and upon releasing the mouse button, the blob is hidden from view. The user can also examine the activation strengths with respect to connectivity. A menu allows the user to choose to view all connections, positive connections, and negative connections. By choosing to view only positive connections, for example, the user will see only the regions whose synaptic activation receives some (or only) excitation; regions with no positive connections (such as SNr) will not be highlighted. Similarly, choosing to view only regions receiving inhibition will result in highlighting regions receiving some (or only) inhibition. It is with this option that SNr's activation will be displayed.

2.4.4 Synthetic PET for Grasp Control

Chapter 2.1 introduced the FARS (Fagg-Arbib-Rizzolatti-Sakata) model of parietal-premotor interactions in grasping. The model focuses on the roles of several intra-parietal areas (AIP, anterior; PIP, posterior; and VIP, ventral intra-parietal), inferior premotor cortex (F4 and F5), presupplementary motor area (F6), frontal cortex (area 46), dorsal premotor cortex (F2), inferotemporal cortex (IT), the secondary somatosensory cortex (SII), and the basal ganglia (BG). However, in this chapter we focus on the contributions of AIP, F5, F6, F2, and the BG.

Model Description

Here we go beyond the description provided in Chapter 2.1 to note that the *current context* used by F5 to select among available grasps may include task requirements, position of the object in space, and even obstacles. When the precise task is known ahead of time, it is assumed that a higher level planning region predisposes the selection of the correct grasp. In the FARS model, it is area F6 that performs this function. However, we can also imagine a task in which the grasp is not known prior to presentation of the object and is only determined by an arbitrary instruction stimulus made available during the course of the trial (e.g., an LED whose color indicates one of two grasps). The dorsal premotor cortex (F2) is thought to be responsible for the association of arbitrary instruction stimulus (IS) with the preparation of motor

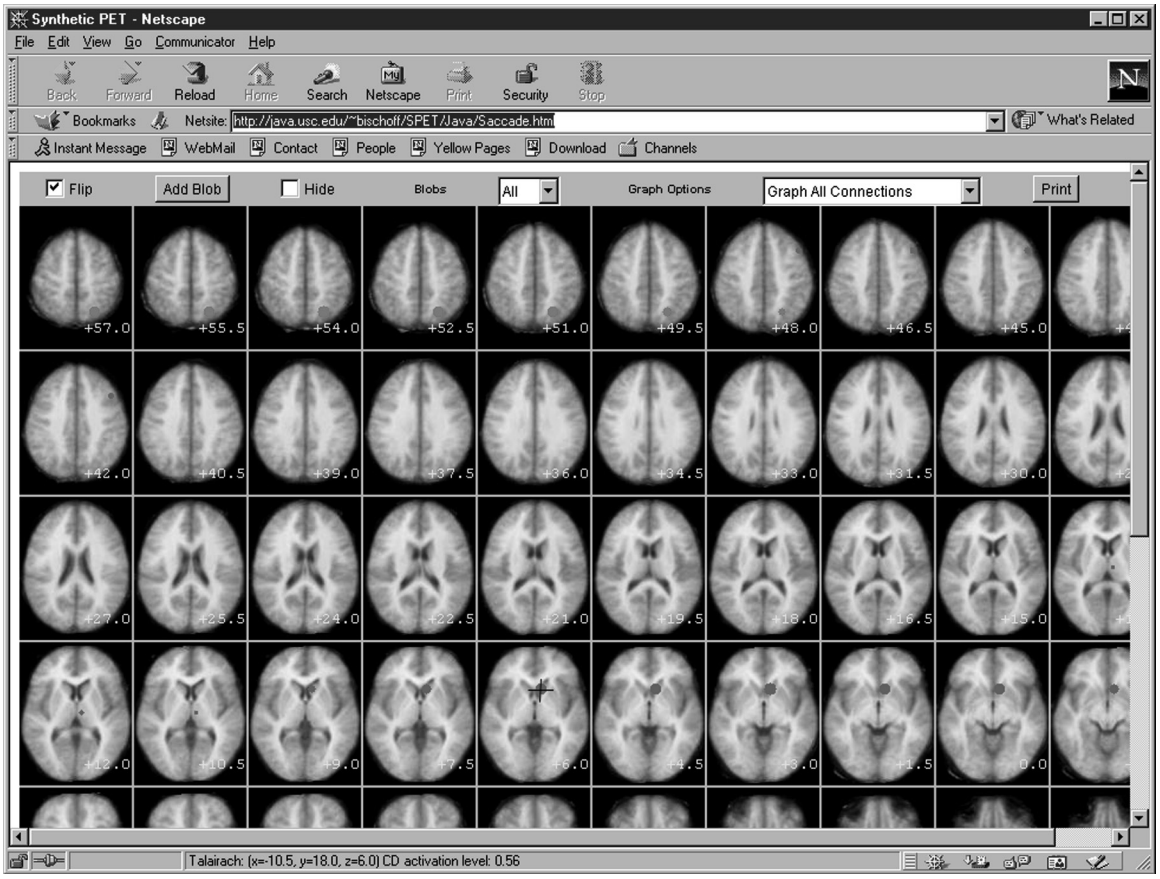

Figure 3 An example showing the crosshair (on slice Z = +6.0) aligned over an activation blob generated by the saccade model. The message bar on the browser provides information regarding the Talairach location of the crosshair. It also indicates that it is aligned over a blob, in this case the caudate (CD), with a relative activation level of 0.56 out of a possible 1.0 score. (See color plates).

programs (Evarts *et al.*, 1984; Kurata and Wise, 1988; Wise and Mauritz, 1985). In a *conditional task* in which a monkey must respond to the display of a pattern with a particular movement of a joystick, some neurons in F2 respond to the sensory-specific qualities of the input, but others specifically encode which task is to be executed on the basis of the instruction—they thus form *set cells* which encode the motor specification until the go signal is received (Fagg and Arbib, 1992; Mitz *et al.*, 1991). We therefore implicate F2 as a key player in this grasp association task. What is particularly interesting about this type of conditional task is that alone neither the view of the object (with its multiple affordances), nor the IS is enough to specify the grasp in its entirety. The visual input specifies the details of all the possible grasps; the IS specifies only the grasp mode—and not the specific parameters of the grasp (such as the aperture). F5 must combine these sources of information in order to determine the unique grasp that will be executed.

Fig. 4a presents an outline of the neural regions involved in the FARS model of grasp production. The precision pinch and power grasp pools of AIP receive inputs from both the dorsal and ventral visual pathways (pathways not shown; more details may be found in Fagg and Arbib, 1998). The pools in F5 and AIP are connected through recurrent excitatory connections. Affordances represented by populations of units in AIP excite corresponding grasp cells in F5; active F5 units, representing a selected grasp, in turn support the AIP units that extract the motorically relevant features of the objects. In monkey, the number of neurons in F5 involved in the execution of the precision pinch is greater than the number observed for any other grasp (Rizzolatti *et al.*, 1988). The model reflects this distribution in the sizes of the precision and power pools in *both* F5 and AIP.

When the model is presented with a conditional task in which the choice of grasp depends on which IS was recently presented, how is a unique grasp selected for execution? According to the FARS model, AIP first extracts the set of affordances that are relevant for the presented object (say, a cylinder). These affordances, which also encode the diameter of the cylinder, activate the corresponding *motor set* cells in F5; however, because there are multiple affordances, several competing subpopulations of F5 set cells achieve a moderate level of activation. This competition is resolved only when the IS is presented. This instruction signal, mapped to a grasp mode preference by the basal ganglia (connections

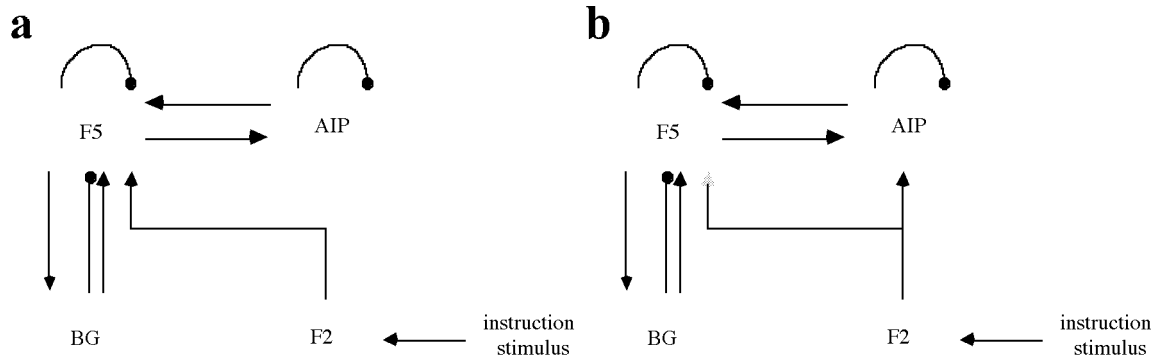

Figure 4 **(a)** A schematic view of the FARS model's architecture. Arrows indicate excitatory connections between regions; filled circles indicate inhibitory connections. The precision pinch and power grasp pools in F5 and AIP are connected through recurrent excitatory connections. The precision pinch pool contains more neurons than other grasps, which affects the Synthetic PET measure in these and downstream regions. F6 represents the high-level execution of the sequence; phase transitions dictated by the sequence are managed by BG. F2 biases the selection of grasp to execute as a function of the presented instruction stimulus. **(b)** An updated functional model, influenced by comparison of Synthetic PET data with actual PET data. In the revised model, the information from F2 flows (primarily) into the circuit through a projection into AIP. AIP: anterior intra- parietal area; BG: basal ganglia; F2: dorsal premotor cortex; F5: inferior premotor cortex; F6: presupplementary motor area.

not shown in the figure), is hypothesized to arrive at F5 via F2. The signal increases the activation level of those F5 cells that correspond to the selected grasp, allowing them to win the competition over the other subpopulations.

Learning from the Comparison of Synthetic PET and Human PET Results

We have conducted several Synthetic PET experiments with the FARS model to predict what we might expect when PET studies are performed in the human. We describe one of them in which we examine the effects of knowing which grasp to use prior to the onset of recording (non-conditional task), as compared with only being told which grasp to use after a delay period (conditional task). In the latter task, an instruction stimulus in the form of a bi-colored LED informs the subject which grasp should be used. The most significant change in PET activity predicted by the model is the level of activity exhibited by area F2 (dorsal premotor cortex). Its high level of activity in the conditional task is due to the fact that this region is only involved when the model must map an arbitrary stimulus to a motor program. In the non-conditional task, the region does not receive IS inputs, thus its synaptic activity is dominated by the general background activity in the region. The additional IS inputs in the conditional task have a second-order effect on the network, as reflected in small changes in synaptic activity in F5, BG, and AIP. There is increased synaptic activity in F5 due to the additional positive inputs from F2. These inputs also cause an increase in the region's *activity level*, which is passed on through excitatory connections to both AIP and BG (recall Fig. 4a).

The Synthetic PET experiments were tested in human PET (see Grafton *et al.*, 1998, for details of the protocol and conditional task results). Subjects were asked to repeatedly perform grasping movements over the 90-second scanning period. The targets of grasping were mounted on the experimental apparatus shown in Fig. 5. Each of three stations mounted on the apparatus consisted of both a rectangular block that could be grasped using a power grasp and a pair of plates (mounted in a groove on the side of the block; see inset of Fig. 5), which could be grasped using a precision pinch (thumb and index finger). A force-sensitive resistive (FSR) material, mounted on the front and back of the block, detected when a solid power grasp had been established. The two plates were attached to a pair of mechanical microswitches, which detected when a successful precision pinch had been executed. For each station, the block and plates were mounted such that the subject could grasp either one without requiring a change in wrist orientation. A bi-colored LED at each station was used to instruct the subject as to the next target of movement. A successful grasp of this next target was indicated to the subject by a change in the color of the LED. The subject then held the grasp position until the next target was given. Targets were presented every $3 +/-0.1$ seconds.

Four different scanning conditions were repeated three times each. In the first, subjects repeatedly performed a power grasp to the indicated block. The target block was identified by the turning on of the associated LED (green in color). When the subject grasped the block, the color of the LED changed from green to red. For the second condition, a precision pinch was used. The target was identified in the same manner as the first condition. In the third grasping condition (conditional task), the initial color of the LED instructed the subject

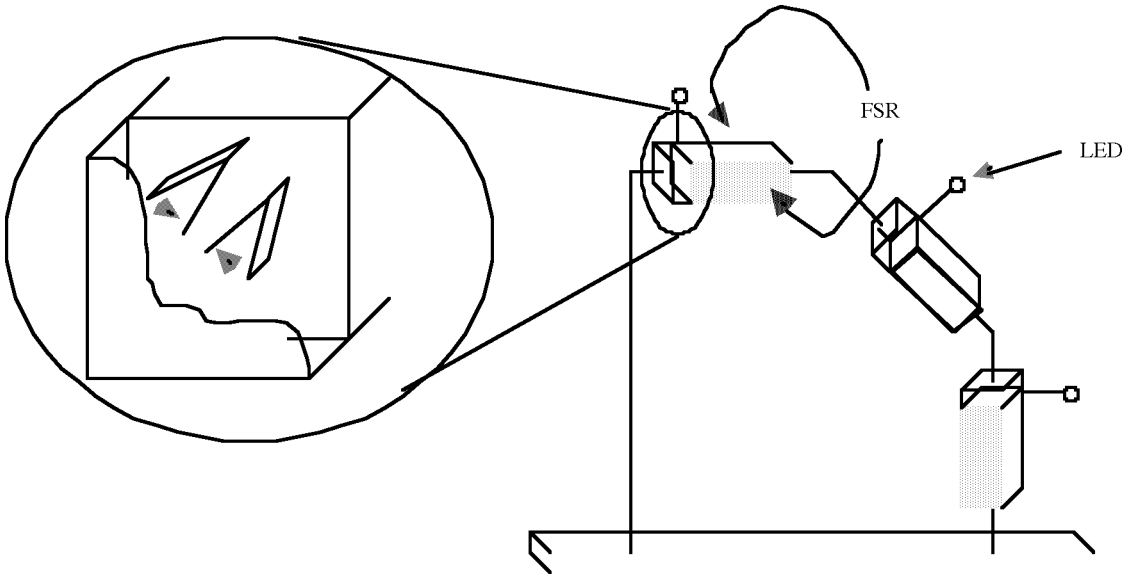

Figure 5 Apparatus used in PET experiment. Each of three stations can be grasped in two ways: precision pinch of the two plates in the grove (inset) or power grasp of the block. The side of the blocks are covered with a force-sensitive resistive (FSR) material; light-emitting diodes (LEDs), depending upon the task, indicate both the goal and type of grasp.

to use either a precision pinch (green) or a power grasp (red). When contact was established, the LED changed to the opposite color. In the fourth (control) condition, the subjects were instructed to simply fixate on the currently lit LED and not make movements of the arm or hand (prior to the scan, the arm was placed in a relaxed position). The lit LED changed from one position to another at the same rate and variability as in the grasping tasks. Prior to scanning, subjects were allowed to practice the tasks for several minutes.

Conditional vs. Non-Conditional Task

The model predicts that the conditional task should yield much higher activation in F2, some activation of F5, and a slight activation of AIP. The human experiment confirmed the F2 result but failed to confirm the predictions for F5. Furthermore, in human we see an activation of the inferior parietal cortex, along the intra-parietal sulcus, which is perhaps an AIP homologue.

Can we make use of the negative F5 result to further refine the model? Consider the functional connectivity of these regions in the model (Fig. 4a). In the model, the strength of the projection from F2 to F5 is essentially a free parameter. In other words, there is a wide range of values over which the model will correctly perform the conditional and non-conditional tasks. The implication is that, by tuning this parameter, we can control this projection's contribution to the synaptic activity measure in F5. However, the difference in AIP synaptic activity from the non-conditional to the conditional task will always be less than the difference observed in F5. Why is this the case? By increasing the projection strength from F2 to F5, we observe an increase in both F5 synaptic *and* cell activity. The increase in F5 cell activity, however, is attenuated by local, recurrent inhibitory connections. Thus, the excitation that is then passed on to AIP via F5 does not reflect the full magnitude of the signal received from F2.

The conclusion is that, although we can adjust the free parameter to match one or the other observations in the human experiment (of either F5 or AIP changes), the model cannot reflect both at the same time. One possibility for repairing this problem in the model is to reroute the F2 information so that it enters the grasp decision circuitry through AIP (or both AIP and F5), rather than exclusively through F5 (Fig. 4b). This would yield an increase in activity in AIP due to F2 activation with only an attenuated signal being passed on to F5, resulting in only a small increase in F5 synaptic activity. Note that we do not necessarily assume that there exists a direct cortico-cortical connection from F2 to AIP or F5, but only that there is a functional connection (which potentially involves multiple synapses).

The low-level details of the FARS grasping model (Fagg and Arbib, 1998) were derived primarily from neurophysiological results obtained in monkey. The synthetic PET approach extracts measures of regional synaptic activity as the model performs a variety of tasks. These measures are then compared to rCBF (regional cerebral blood flow) observed during human PET experiments as the subjects perform tasks similar to those simulated in the model. In some cases, the human results provide confirmation of the model behavior. In other cases, where there is a mismatch between model prediction and human results, it is possible (as we have

shown) to use these negative results to further refine and constrain the model and, on this basis, design new experiments for both primate neurophysiology and human brain imaging.

2.4.5 Discussion

The Synthetic PET methodology allows users to make specific predictions in PET experiments based upon neural network models of behavior. Because models typically rely upon neurophysiology, neuroanatomy, and behavioral data, Synthetic PET provides a way of bridging the gap between different temporal resolutions; models can be compared with actual PET studies of the same kind. This allows the modeler to further validate his research and can provide suggestions for experimentalists for future research regarding a particular phenomenon. It also provides a way to separate the contributions of positive and negative connections, a powerful method towards the understanding of the contribution of individual regions to another area's overall activation level.

Our current implementation of Synthetic PET focuses upon coloring the Talairach Atlas with elliptical blobs. In the future, we plan to add other atlases, such as rat or monkey, to its functionality. PET is increasingly used in research with nonhuman primates; the Synthetic PET method would then provide another method of analysis in comparing models based upon monkey data to the data gathered with conventional PET. Furthermore, we plan to add the capability of generating a Synthetic PET image based directly upon single-unit recordings. While the activation generated would be limited to the regions which were recorded, it will still provide a way of examining how neurons with different temporal characteristics can contribute to the activation of a region under a particular paradigm. As described in Chapters 3.1 and 3.2, the NeuroCore database stores neurophysiological data and includes features for manipulation of these data. Synthetic PET would be able to connect with the data and would contain the routines necessary for calculating blobs of activation.

We plan to improve our algorithm in the future for the modeling of fMRI data as well. This would provide yet another link to the neurophysiological data by presenting us with a visual time course of activation changes. The current Synthetic PET technique is based upon the hypothesis that PET is correlated to the integrated synaptic activity within a region. Both to improve our Synthetic PET algorithms and to develop Synthetic fMRI, we will have to investigate possible correlates with neural firing and synaptic plasticity, as well as synaptic activity. We must also note that we will need to extend our basic neural models to better understand the link between blood flow (hemodynamics), neural metabolism, and the information processing role of these neurons. Further, we plan to improve our representation of activation from that of an ellipsoid to one which more closely corresponds to the shape of the region under study. This will improve the conditions of comparing Synthetic PET/fMRI to conventional PET/fMRI. By representing the region's shape itself within the database, it becomes possible to be more specific as to the location of the activation (e.g., ventrolateral pallidum as opposed to the entire pallidum will be highlighted). However, it is worth stressing that as a region becomes more active the increase of the active area we see in its image may not reflect an increase of the population of neurons engaged in the activity so much as the increased rCBF in regions through which blood vessels pass en route to the activated region. We also need to add a stochastic analysis to account for the variation in PET activity seen in the same subject on different trials.

The current implementation of Synthetic PET is stand-alone in that it does not interface with the NSL environment (Chapter 2.2). Future development plans include providing crosstalk between the two programs. For example, a user running an experiment in NSL should be able to link the model's results to a Synthetic PET image upon completion of the experiment. The information required by Synthetic PET should be part of a NSL program and its results; our current implementation involves manually calculating and entering the required information into the database.

Finally, Synthetic PET only displays brain slices and a blob of activity related to a given region's activation. In Arbib *et al.* (1995) we used a line graph to illustrate activation differences between two tasks. Within Synthetic PET, a click of a button would display this graph in a separate window so that the current task may be compared to another task's results (such as simple vs. memory saccades, or internally vs. externally guided motor sequencing). We could thus view the material in three forms (returning to the saccade model for these particular figures): integration over inhibitory connections (Fig. 6a; see color insert), over excitatory connections (Fig. 6b; see color insert), and over all connections (Fig. 6c; see color insert). This kind of presentation allows us to refer back to the simulation to infer reasons for the results which may seem contradictory when the PET values are related to total cell firing in a region (reflecting the *difference* between excitatory and inhibitory input) as opposed to the *summed* contributions of the absolute values of the excitatory and inhibitory inputs. For example, the negative activity in the thalamus decreases when comparing simple saccades to memory saccades, while the positive activity strongly increases; overall, however, there is a decrease in synaptic activity in MD thalamus when both positive and negative connections are considered. In order to generate a graph illustrating the connections, the user merely presses a button labeled "Graph Activity." This will

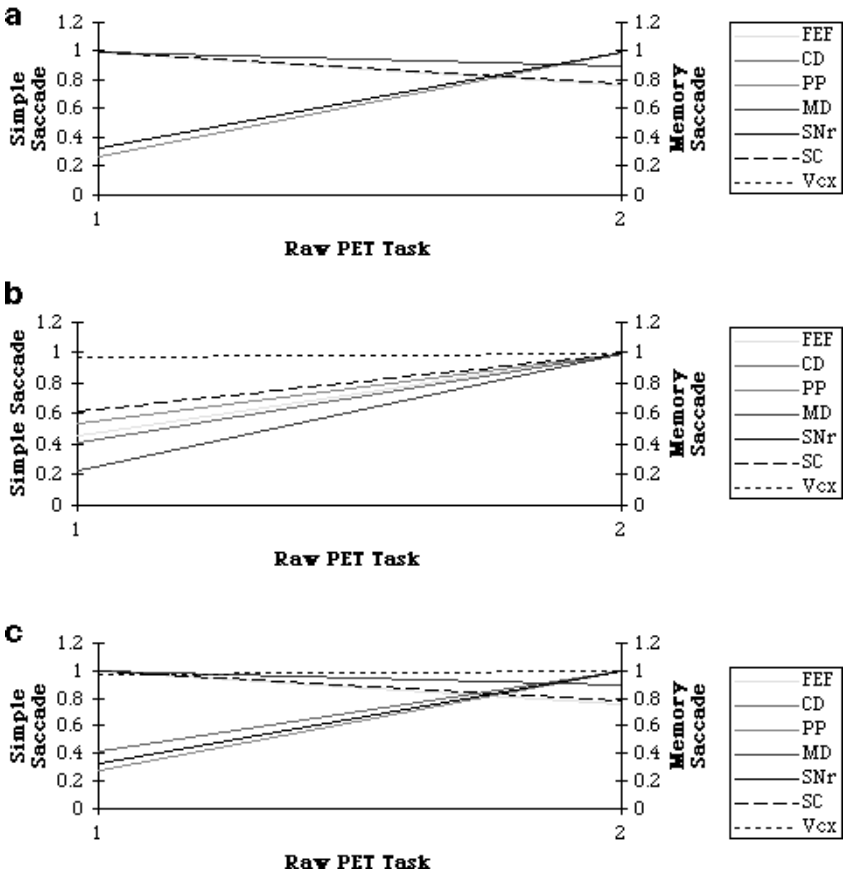

Figure 6 The raw activity $rPET_a$ associated with each cell group A in the neural network model for saccade generation obtained by integrating: **(a)** over inhibitory connections, **(b)** over excitatory connections, and **(c)** over all connections. Left column: $rPET_a$ values for the simple saccade task. Right column: values for the memory saccade task. Note that in B, CD and Vcx coincide, as do SC and FEF. Similarly, FEF and SC coincide in C. CD: caudate; FEF: frontal eye fields; PP: posterior parietal cortex; SC: superior colliculus; SNr: substantia nigra pars reticulata; MD: mediodorsal thalamus; Vcx: visual cortex. (see color plates.)

display a Matlab graph similar to that seen in Fig. 6 (see color insert).

As a fully developed tool, Synthetic PET will allow experimenters to integrate data collected via various methods. With the Neuroinformatics Workbench supplying techniques for storing both modeled, behavioral, and neurophysiological data, Synthetic PET allows us to link the various aspects of our database together. As we have seen with the saccade example, results can be counterintuitive, as the predictions are based upon both excitatory and inhibitory synaptic activity. In the future, an imaging database will provide yet another method of comparing modeled and physiological data with that collected by PET or fMRI methodologies. This would make it possible to determine if PET activation seen is largely based upon excitatory or inhibitory synaptic activity. Finally, Synthetic PET is a method that allows interaction between researchers within the neurosciences who share interests in a particular behavior and strive for a more rigorous understanding of the hypothesized homologies across species.

References

Ackermann, R. F., Finch, D. M., Babb, T. L. and Engel, J. J. (1984). Increased glucose metabolism during long-duration recurrent inhibition of hippocampal pyramidal cells. *J. Neurosci.* **4**, 251–264.

Arbib, M. A., Bischoff, A., Fagg, A. H. and Grafton, S. T. (1995). Synthetic PET: analyzing large-scale properties of neural networks. *Human Brain Mapping* **2**, 225–233.

Brownell, G. L., Budinger, T. F., Lauterbur, P. C. and McGeer, P. L. (1982). Positron tomography and nuclear magnetic resonance imaging. *Science* **215**, 619–626.

Dominey, P. F., and Arbib, M. A. (1992). A cortico-subcortical model for generation of spatially accurate sequential saccades. *Cerebral Cortex* **2**, 153–175.

Evarts, E. V., Shinoda, Y., and Wise, S. P. (1984). *Neurophysiological Approaches to Higher Brain Function*. Wiley-Interscience Press, New York.

Fagg, A. H., and Arbib, M. A. (1998). Modeling parietal-premotor interactions in primate control of grasping. *Neural Networks* **11**, 1277–1303.

Fagg, A. H., and Arbib, M. A. (1992). A model of primate visual-motor conditional learning. *J. Adaptive Behav.* **1**, 3–37.

Grafton, S. T., Fagg, A. H. and Arbib, M. A. (1998). Dorsal premotor cortex and conditional movement selection: a PET functional mapping study. *J. Neurophysiol.* **79**, 1092–1097.

Herscovitch, P., Markham, J. and Raichle, M. (1983). Brain blood flow measured with intravenous $H_2{}^{15}O$. I. Theory and error analysis. *J. Nuclear Med.* **24**, 782–789.

Hikosaka, O., and Wurtz, R. H. (1983a). Visual and oculomotor functions of monkey substantia nigra pars reticulata. I. Relation of visual and auditory responses to saccades. *J. Neurophysiol.* **49**, 1230–1253.

Hikosaka, O., and Wurtz, R. H. (1983b). Visual and oculomotor functions of monkey substantia nigra pars reticulata. III. Memory continent visual and saccade responses. *J. Neurophysiol.* **49**, 1268–1284.

Kurata, K., and Wise, S. P. (1988). Premotor cortex of rhesus monkeys: set-related activity during two conditional motor tasks. *Exp. Brain Res.* **69**, 327–343.

Mitz, A. R., Godshalk, M. and Wise, S. P. (1991). Learning-dependent neuronal activity in the premotor cortex. *J. Neurosci.* **11**, 1855–1872.

Raichle, M. E., Martin, W. R. W. and Herscovitch, P. (1983). Brain blood flow measured with intravenous $H_2{}^{15}O$. II. Implementation and validation. *J. Nucl. Med.* **2**, 790–798.

Rizzolatti, G., Camarda, R., Fogassi, L., Gentilucci, M., Luppino, G. and Matelli, M. (1988). Functional organization of inferior area 6 in the macaque monkey. II. Area F5 and the control of distal movements. *Exp. Brain Res.* **71**, 491–507.

Talairach, J., and Tournoux, P. (1988). *Co-planar Stereotaxic Atlas of the Brain*. Thieme Medical Publishers, New York.

Wise, S. P., and Mauritz, K. H. (1985). Set-related neuronal activity in the premotor cortex of rhesus monkeys: effects of changes in motor set. *Proc. R. Soc. London.* **223**, 331–354.

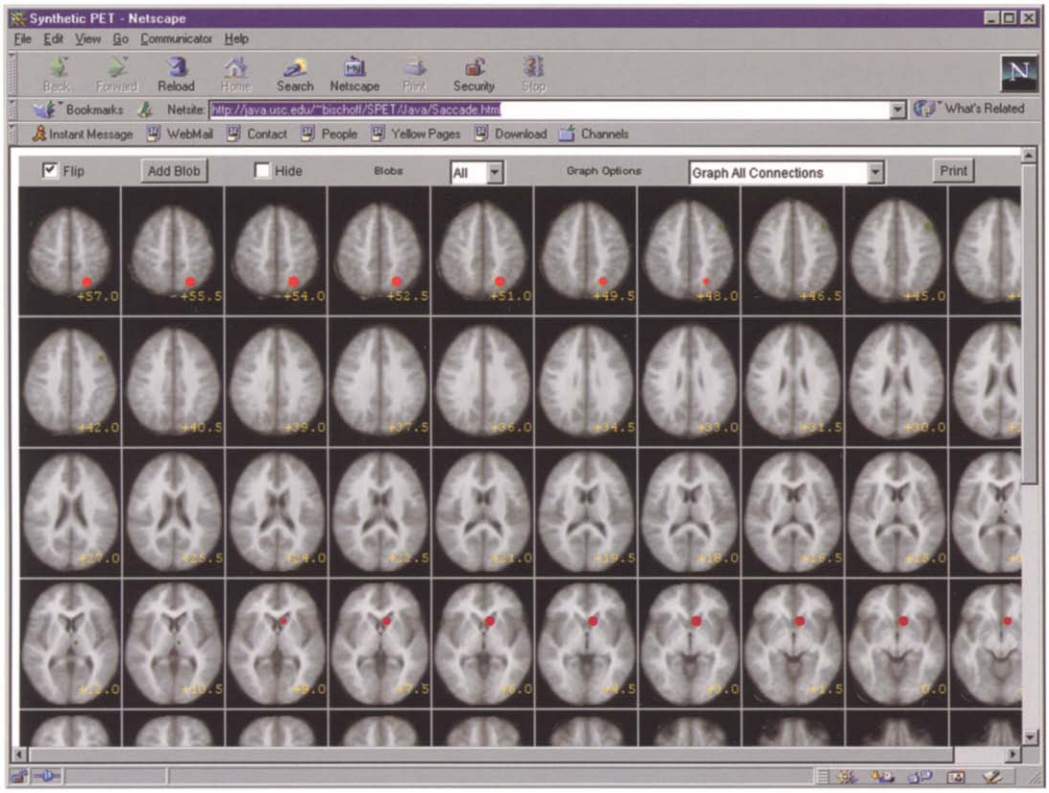

CHAPTER 2.4, FIGURE 2 Synthetic PET comparison generated for the saccadic movement model. The top portion of the frame provides a checkbox for flipping the atlas orientation, adding new blobs, viewing or hiding specific blobs, and for choosing graph options. In the saccade example, we have chosen to view all the blobs and activation changes related to both positive and negative synaptic input. Red activation: overall increase in activity. Green activation: overall decrease in activity.

CHAPTER 2.4, FIGURE 3 An example showing the crosshair (on slice $Z = +6.0$) aligned over an activation blob generated by the saccade model. The message bar on the browser provides information regarding the Talairach location of the crosshair. It also indicates that it is aligned over a blob, in this case the caudate (CD), with a relative activation level of 0.56 out of a possible 1.0 score.

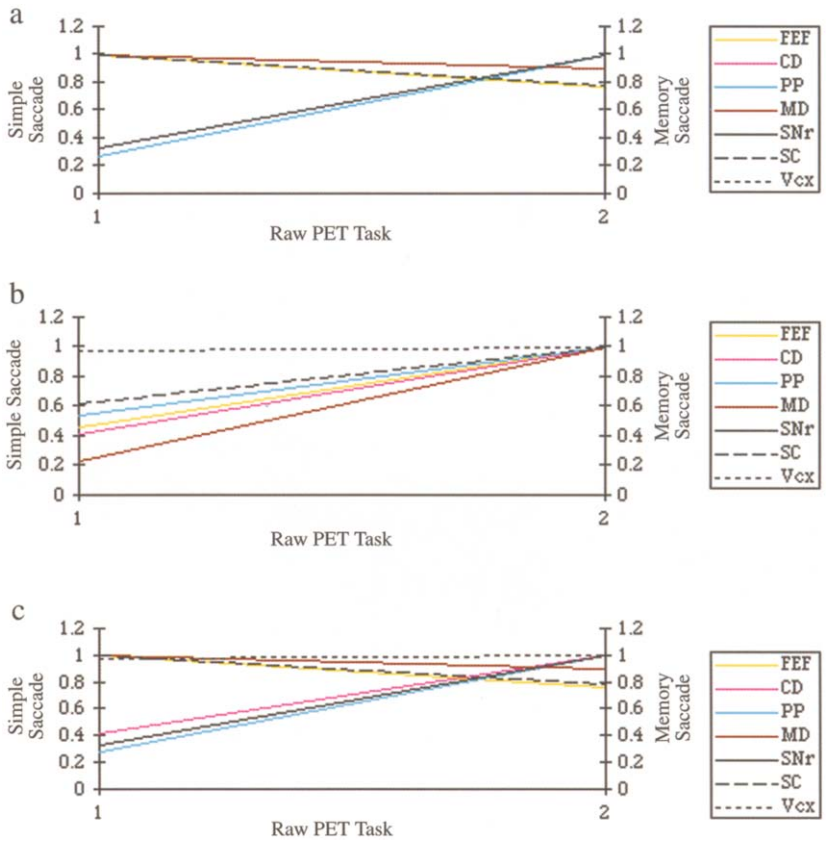

CHAPTER 2.4, FIGURE 6 Simple vs. memory saccade-related raw activity $rPET_A$ associated with each cell group A in the neural network model for saccade generation obtained by integrating: (a) over inhibitory connections; (b) over excitatory connections; and (c) over all connections. Left column: $rPET_A$ values for the simple saccade task. Right column: values for the memory saccade task. Note that in B, CD and Vcx coincide, as do SC and FEF. Similarly, FEF and SC coincide in C. CD, caudate; FEF, frontal eye fields; PP, posterior parietal cortex; SC, superior colliculus; SNr, substantia nigra pars reticulata; MD, mediodorsal thalamus; and Vcx, visual cortex.

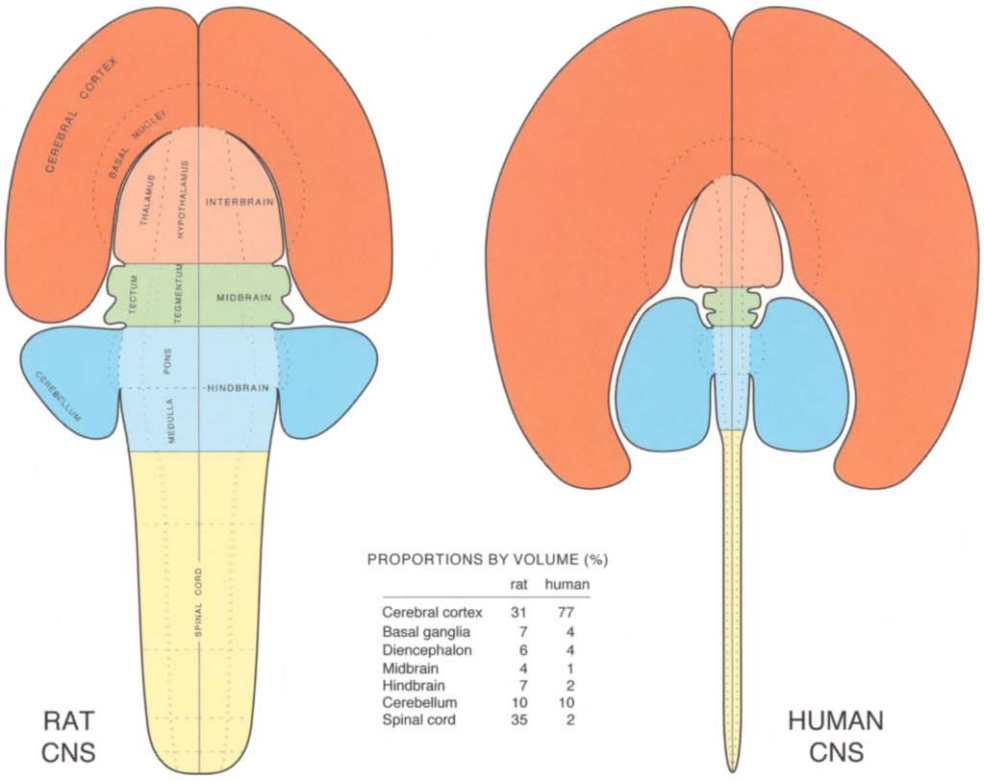

CHAPTER 4.1, FIGURE 5 Flatmaps of the rat (left) and human (right) central nervous system. For simplicity, the *volume* of structures in the actual brain are proportional to their *area* in the schematic flatmap. The table in the center of the figure compares the size of major central nervous system divisions between rat and human. See text for further details. (From Swanson, L.W. (1995) *Trends Neurosci.* **18**, 471–474. With permission from Elsevier Science.)